Proceedings of IMECE2006
2006 ASME International Mechanical Engineering Congress and Exposition
November 5-10, 2006, Chicago, Illinois, USA

IMECE2006-14870

Vision-Based Kinematic Synthesis of Hand Motion

Karthikeyan Duraisamy
Measurement and Controls Engineering Research Center (MCERC)
College of Engineering
Idaho State University
Pocatello, ID 83209

Alba Perez-Gracia
Measurement and Controls Engineering Research Center (MCERC)
College of Engineering
Idaho State University
Pocatello, ID 83209

Marco P. Schoen
Measurement and Controls Engineering Research Center (MCERC)
College of Engineering
Idaho State University
Pocatello, ID 83209

ABSTRACT

The purpose of this work is to develop a human hand model that will work in conjunction with the myoelectric signals from the arm muscles, for those people who have lost their upper extremity. Though there are many prostheses available on the market with variable cost and functional accuracy, it is hard to find a prosthesis that mimics the complete functionality of the human hand, due to the complex hand motion, the complex dynamics of the myoelectric signals, and the difficulty involved in the acquisition of these signals, which complicates the implementation. In order to overcome some of these problems, the proposed hand model mimics most of the hand movements and it is used together with a kinematic synthesis process to identify the motion of the hand, obtained from visual data.

In this paper, the human hand is modeled as a collection of five serial chains. For each movement performed by the joints in the finger/wrist, revolute joints are considered in different configurations, which yield movements similar to those of the human hand. The forward kinematics in matrix form is formulated using Denavit-Hartenberg parameters and expressed using Clifford Algebra exponentials. Kinematic synthesis is used to adjust the dimensions of the proposed model to the hand of the subject, and to identify the angles at each joint for a given hand motion. In the kinematic synthesis process, the forward kinematics equations of the hand are solved for both the angles of the joints and the dimensions of the hand.

The synthesis equations obtained from the kinematic synthesis process are solved using a Levenberg-Marquardt nonlinear least-squares algorithm. The experimental setup for the real-time motion capturing consists of three camerasand is to be used in future work to relate the joint motion to the myoelectric signals acquired from the subject's arm.

INDEX TERMS –Kinematic synthesis, Clifford algebra, motion capture, hand prosthesis Levenberg-Marquardt least-squares algorithm

1. INTRODUCTION

Commercially available upper-body prosthetic devices have seen little improvement in terms of functionality and ability since World War II. While the development for leg and foot prosthetic devices has enjoyed much attention due to the higher number of incidents such as foot amputation due to diabetic neuropathy, hand prosthetics lack in availability and functionality. Research in developing smart or intelligent artificial hands is a very active field of research. Most of the solutions use robotic hands actuated by myoelectric signals. Myoelectric signal is the term given to the nerve impulse that travels from the brain to a muscle and initiates action. Even though an individual's appendage is gone, the body is still able to convey the nerve impulses that excited the muscles of the missing appendage.

Most of the ongoing research aims to identify and control a set of basic motions. Zhao et al [1] developed a five-fingered underactuated prosthetic hand system, which uses variable learning rate (VLR) neural networks with autoregressive (AR) and wavelet parameters to discriminate the EMG signals for a set of grasping and other basic motions. Zollo et al. [2] and Cipriani et al. [3] present designs of anthropomorphic hands to be applied in prosthetics, with control and feedback formulated to imitate common hand tasks. Bitzer and Van der Smagt [5] present the control of three fingers of a four-fingered hand using EMG signals, which they relate to binary flexion-extension motion. Research in identifying hand motion is also a very active field of research, both for biomedical applications and for virtual reality and computer graphics. Koshino and Tanimoto [4] present a method to estimate hand postures from visual data matching the captured image to a database of postures. Veber and Bajd [6] used hand images to compute the inverse kinematics of the hand, but they simplify it to a planar motion. In our approach [7], each finger is described as a serial robot expressed as Clifford Algebra exponentials, which allows us to perform kinematic synthesis to obtain the angles at each

joint and to adapt the model to the dimensions of the hand of the subject being captured, with the visual data obtained from the motion tracking system. The kinematic model so obtained quantifies the motion of the natural hand.

The anatomy of the human hand is briefly presented in section 2, and the kinematic modeling of the hand is introduced in section 3. Section 4 shows the detailed explanation of the kinematic synthesis and tracking for the hand model. The synthesis results using Levenberg-Marquardt nonlinear least squares algorithm are presented in section 5. Then the motion tracking (section 6) and conclusions (section 7) are presented.

2. THE HUMAN HAND

The skeleton of the hand consists of 27 bones. Eight of them are carpal bones, organized in two rows of proximal and distal carpal bones. The other 19 are long bones, which extend in five rays (polyarticulated serial chains), are made of metacarpal bones and phalanges (proximal, middle and distal). The wrist consists of the radial and ulna bones.

Joints are formed at the surface of relative motion between two bones. For some of the joints, their motion can be approximated to that of the revolute joint, even though the real motion is more complicated and requires the model of the matching surfaces. Some other joints can perform motion in different directions and can be modeled as two degree-of-freedom joints.

The joints considered are: radiocarpal joint at the wrist, carpo-metacarpal (CMC) joint between the distal carpal row and the metacarpal bone, metacarpal-phalangeal joint (MCP) between metacarpal and proximal phalange bone, and proximal and distal interphalangeal joints (PIP, DIP) separating the phalangeal bones. See Figure 1.

The range of motion of each joints and the dimensions and type of joints for our simulations were taken from several sources [8], [9], [10] that present some variability in their numerical values.

A. Wrist and carpal Motion

The wrist movement includes flexion/extension, adduction/abduction and the circular motion that is created at the lower arm. This is a total of three DOF that are common to all the fingers.

B. Index and Middle Fingers

The index and the middle fingers are also called radial digits, and have a similar motion: flexion, extension and certain degree of adduction and abduction at the MCP joint. Movement at the CMC joint is negligible, which gives these two fingers a total of four degrees of freedom each. See Fig.1 (II & III)

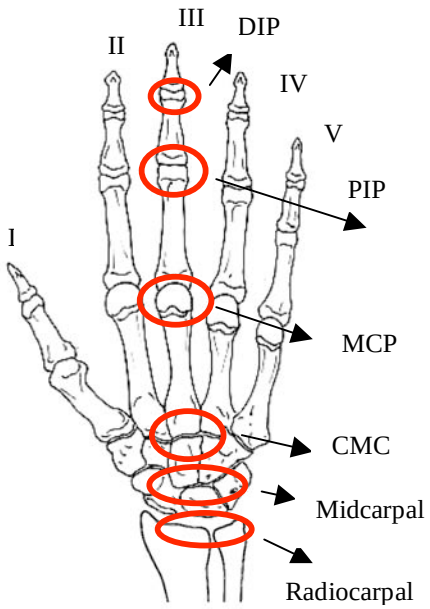

Fig.1 Posterior view of hand joints

C. Ring and Little Fingers

The ring and little fingers are also called the ulna digits. They have the same features as the index and middle fingers, but with greater mobility at the CMC joint, which cannot be neglected. This gives five degrees of freedom to each of them. See Fig.1 (IV & V)

D. Thumb Finger

The thumb has a greater range of motion than the other fingers, and its joints present a more complex motion. The bones that are responsible for thumb movement are: scaphoid, trapezium, first metacarpal, proximal and distal phalanges. All these bones give a total of five degrees of freedom to the thumb. The CMC joint is a biaxial joint (sellar/saddle joint) that performs flexion/extension and adduction/abduction. The MCP joint is a condyloid joint (biaxial joint). There is flexion/extension, adduction/abduction and a slight rotation that we can neglect. The distal interphalangeal joint is a hinge joint more similar to those of the other fingers that presents one degree of freedom. See Fig.1 (I)

3. KINEMATIC MODELING OF THE HUMAN HAND

3.1. Introduction

A kinematic model of the human hand has been developed in order to track independently the motion of each degree of freedom. Each of the fingers is modeled as a serial kinematic chain composed of revolute joints.

Most of the actual motion-tracking models represent the motion using spherical joints, that is, an arbitrary rotation located at a point. Even though that model gives fast results, it does not capture the actual structure of the skeleton so precisely, where the rubbing surfaces create joints with well-defined joint axes in many cases. It also increases the number of parameters to track. A different type of research [13] is

directed to model the rubbing surfaces of the bones, obtaining a very detailed, yet computationally expensive description of the joint motion. Unlike these two approaches, we model the joints as revolute or universal joints. This allows us to have a precise description of the motion with less joint parameters, as well as to have a more defined description of the kinematics structure, without a very high computational load.

Clifford algebra exponentials are used to represent the motion at each joint, expressed as relative motion from a reference configuration. The total displacement is obtained by composing the motion about each consecutive joint.

In order to be able to properly track the motion of the subject, we need to adapt the dimensions and morphology of the generic hand model to that of the individual being studied. For doing so, we use the visual data to perform kinematic synthesis, which includes the inverse kinematics. Once the model of the hand is adapted to that of the individual, only the inverse kinematics, or motion tracking, is needed.

3.2. The Kinematics Equations of a Serial Chain

The Kinematics equations for a serial chain define the position of its end-effector as a function of the geometry of the chain and the joint variables. They can be expressed as a product of local displacements using the link length and twist angle between consecutive joints, a_{ij} and α_{ij}, and the rotation (joint angle) and translation (offset) about each joint, θ_i and d_i; these parameters are known as the Denavit-Hartenberg parameters. Consider the serial chain defined by several joint axes as in Fig. 2. For the m-jointed kinematic chain, the kinematics equations, expressed as homogeneous transformations, are

$$[D_i] = [G][Z(\theta_0^i, d_0^i)][X(\alpha_{01}, a_{01})][Z(\theta_1^i, d_1^i)]\ldots$$
$$[X(\alpha_{n-1}, a_{n-1}, n)][Z(\theta_m^i, d_m^i)][H],\ \text{i=1,...n,} \tag{1}$$

where $[G]$ locates the base of the chain with respect to the fixed reference frame F, and $[H]$ represents the displacement between the end-effector and the last joint m.

Similarly, the relative motion with respect to a reference configuration $[D_0]$, is given by $[D_{oi}] = [D_i][D_o]^{-1}$.

The relative displacement equations take the form

$$[D_{oi}(\Delta\vec{\theta}^{\,i})] = [T(\Delta\theta_0^i, S_0)][T(\Delta\theta_1^i, S_1)]$$
$$\ldots[T(\Delta\theta_m^i, S_m)], \tag{2}$$

The matrix $[T(\Delta\theta_j^i, S_j)]$ represents a screw displacement about the joint axis S_j. These are expressed in the fixed frame and at the reference configuration using Plucker coordinates, measuring the joint variable j from the reference configuration, $S_j = S_j + \varepsilon S_j^0$ and $\Delta\theta_j^i = \theta_j^i - \theta_j^0$.

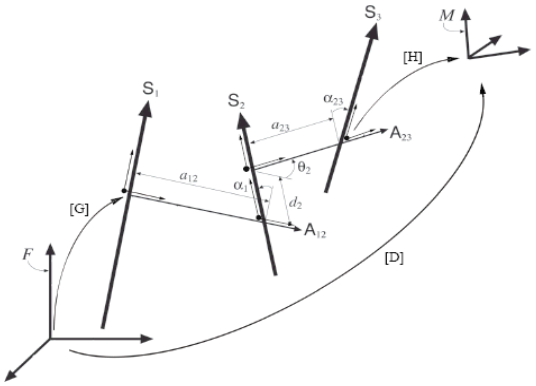

Fig. 2 Generic serial chain with m joints

3.3. Clifford Algebra Kinematics Equations

Instead of using the homogeneous matrix representation, this work uses the Clifford algebra of dual quaternions to express the motion. A relative motion given by a screw axis, angle and slide is easy to express as a dual quaternion, also reducing the total number of parameters used to define the motion. This provides a systematic and compact way of writing the equations of relative motion of serial chains.

The Clifford algebra of the projective three-space P^3 is a sixteen-dimensional vector space with a non-commutative product called geometric or Clifford product [11]. The elements of even rank form an eight-dimensional sub-algebra $C^+(P^3)$ that can be identified with the set of $4x4$ homogeneous transforms.

Consider $s = s_1 i + s_2 j + s_3 k$ and $s^o = s_5 i + s_6 j + s_7 k$, so that the Clifford algebra element is written as

$$\hat{S} = s_o + s + s_4\varepsilon + s^o\varepsilon$$
$$= (s_o + s_4\varepsilon) + (s + s^o\varepsilon) = \hat{s} + S \tag{3}$$

For more information about the Clifford algebra of dual quaternions used in kinematic synthesis, see [12].

A spatial displacement is identified with the unit dual quaternion obtained as the Clifford algebra exponential of the screw $J = s + \in(cxs + \mu s)$

$$\hat{Q} = e^{\frac{\phi}{2}J} = \cos\frac{\phi}{2} + \sin\frac{\phi}{2}S, \tag{4}$$

where $S = s + \varepsilon(cxs)$ is the screw axis of the displacement, and $\hat{\phi}$ is the dual axis variable defined as $\hat{\phi} = \phi + \varepsilon t$, with t being the translation along and ϕ the rotation about the axis.

The composition of these Clifford algebra elements defines the relative kinematics equations for a serial chain that are

equivalent to $Eq.(2)$ as the product of Clifford algebra exponentials,

$$\begin{aligned}\hat{D}_i(\Delta\hat{\hat{\theta}}) &= \hat{Q}_1(\hat{\theta}_o^i)\hat{Q}_2(\hat{\theta}_1^i)\ldots\hat{Q}_m(\theta_m^i) \\ &= e^{\frac{\Delta\hat{\theta}_{0j}}{2}S_0}e^{\frac{\Delta\hat{\theta}_{1j}}{2}S_1}\ldots e^{\frac{\Delta\hat{\theta}_{nj}}{2}S_{m,}}\end{aligned} \tag{5}$$

Here $\hat{Q}_j(\theta_j^i) = \cos(\frac{\Delta\theta_j^i}{2}) + \sin(\frac{\Delta\theta_j^i}{2})S_j$ corresponds to the relative transformation of the chain about joint j from the reference configuration $\hat{D}_o$.

3.4. The Hand Model

Table 1. D-H parameters for the middle finger

Axis	α	a	d	θ
S_0	0	0	0	θ_0
S_1	$\frac{\pi}{2}$	0	0	$\theta_1+\frac{\pi}{2}$
S_2	$\frac{\pi}{2}$	0	0	θ_2
S_4	$\frac{\pi}{2}$	2.8	0	θ_4
S_5	0	4.3	0	θ_5
S_6	$\frac{\pi}{2}$	0	0	θ_6
S_7	$\frac{\pi}{2}$	3.5	0	θ_7
S_8	0	2.6	0	θ_8

The hand is modeled as five independent serial chains with eight degrees of freedom each. The first three joints, flexion / extension, abduction / adduction and pronation / supination of the radiocarpal joint at the wrist, are common to all five serial chains. According to [21], [22] the wrist articulation is created by the collective action of the radiocarpal joint and the midcarpal joint. Instead of considering joints, our approach considers a single motion at the radiocarpal joint, which incorporates the hand articulation given by the midarpal joint. As a result, the midcarpal joint itself is considered immobile in our hand model. The carpo-metacarpal joint is modeled as a revolute joint; the metacarpo-phalangeal joint is modeled as two revolute joints intersecting at 90 degrees; and the proximal and distal interphalangeal joints are modeled as revolute joints. Table 1 presents the Denavit-Hartenberg parameters that define the middle finger of the hand model.

The kinematic equations, as relative motion from a reference configuration, are given by

$$\begin{aligned}\hat{Q}_{index} &= \hat{S}_{c0}(\theta_0)\hat{S}_{c1}(\theta_1)\hat{S}_{c2}(\theta_2)\hat{S}_{c4}(\theta_4)\ldots \\ &\quad \hat{S}_{c7}(\theta_7)\hat{S}_{c8}(\theta_8) \\ &= (\cos\frac{\theta_0}{2} + \sin\frac{\theta_0}{2}S_{c0})(\cos\frac{\theta_1}{2} + \sin\frac{\theta_1}{2}S_{c1})\ldots \\ &\quad (\cos\frac{\theta_8}{2} + \sin\frac{\theta_8}{2}S_{c8}),\end{aligned} \tag{6}$$

This corresponds to the axes shown in Fig. 3 for the reference configuration.

A rotation about a revolute joint $S = s + \varepsilon s^0$ takes the form, if we write the scalar as the fourth component of the vector,

$$\begin{aligned}\hat{S}(\theta) &= \cos\frac{\theta}{2} + \sin\frac{\theta}{2}S \\ &= \begin{Bmatrix}\sin\frac{\theta}{2}s_x \\ \sin\frac{\theta}{2}s_y \\ \sin\frac{\theta}{2}s_z \\ \cos\frac{\theta}{2}\end{Bmatrix} + \varepsilon\begin{Bmatrix}\sin\frac{\theta}{2}s_x^o \\ \sin\frac{\theta}{2}s_y^o \\ \sin\frac{\theta}{2}s_z^o \\ 0\end{Bmatrix}\end{aligned}$$

The dual quaternion expression of two revolute joints $S_1 = s_1 + \varepsilon(c \times s_1)$ and $S_2 = s_2 + \varepsilon(c \times s_2)$ that intersect at right angles at a point c is somewhat simpler than the product of two general rotations; we denote it by $\hat{T}$,

$$\begin{aligned}\hat{T}_{12}(\theta_1,\theta_2) &= (\cos\frac{\theta_1}{2} + \sin\frac{\theta_1}{2}S_1)(\cos\frac{\theta_2}{2} + \sin\frac{\theta_2}{2}S_2) \\ &= \begin{Bmatrix}s_1 s\frac{\theta_1}{2}c\frac{\theta_2}{2} + s_2 c\frac{\theta_1}{2}s\frac{\theta_2}{2} + s_1 \times s_2 s\frac{\theta_1}{2}s\frac{\theta_2}{2} \\ c\frac{\theta_1}{2}c\frac{\theta_2}{2}\end{Bmatrix} \\ &\quad + \varepsilon\begin{Bmatrix}cx(s_1 s\frac{\theta_1}{2}c\frac{\theta_2}{2} + s_2 c\frac{\theta_1}{2}s\frac{\theta_2}{2} + (s_1 \times s_2)s\frac{\theta_1}{2}s\frac{\theta_2}{2}) \\ 0\end{Bmatrix}\end{aligned} \tag{7}$$

For the index finger, the motion at the carpo-metacarpal joint (S_4) is negligible. The kinematics equations for the index finger is written as

$$\begin{aligned}\hat{Q}_{index} &= \hat{S}_{c0}(\theta_0)\hat{T}_{c12}(\theta_1,\theta_2)S_{i4}(\theta_4)\hat{T}_{i56}(\theta_5,\theta_6) \\ &\quad \hat{S}_{i7}(\theta_7)\hat{S}_{i8}(\theta_8)\end{aligned} \tag{8}$$

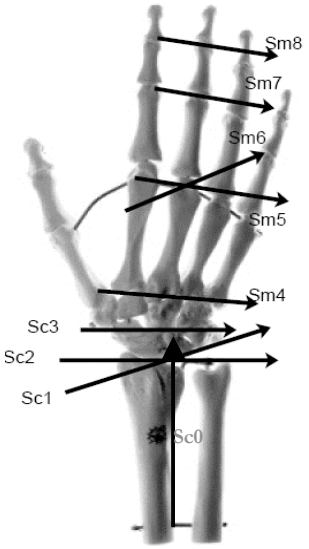

Fig.3. Kinematic model for the middle finger (Illustration from Authentic anatomical™ model)

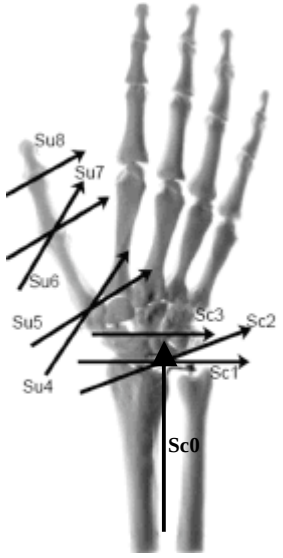

Fig.4. Kinematic model for the thumb finger

The kinematics equations for the middle, ring and little fingers present the same structure,

$$\begin{aligned}\hat{Q}_{middle} &= \hat{S}_{c0}(\theta_0)\hat{T}_{c12}(\theta_1,\theta_2)S_{i4}(\theta_4)\hat{T}_{i56}(\theta_5,\theta_6)\\ &\quad \hat{S}_{i7}(\theta_7)\hat{S}_{i8}(\theta_8)\\ \hat{Q}_{ring} &= \hat{S}_{c0}(\theta_0)\hat{T}_{c12}(\theta_1,\theta_2)S_{i4}(\theta_4)\hat{T}_{i56}(\theta_5,\theta_6)\\ &\quad \hat{S}_{i7}(\theta_7)\hat{S}_{i8}(\theta_8)\\ \hat{Q}_{little} &= \hat{S}_{c0}(\theta_0)\hat{T}_{c12}(\theta_1,\theta_2)S_{i4}(\theta_4)\hat{T}_{i56}(\theta_5,\theta_6)\\ &\quad \hat{S}_{i7}(\theta_7)\hat{S}_{i8}(\theta_8)\end{aligned} \tag{9}$$

It is important to mention here that the motion at the carpo-metacarpal joint (S_4) is negligible in the case of index and middle finger, but not for the ring and little finger.

The thumb is modeled so that the carpo-metacarpal joint consists of two intersecting revolute joints, same as the meta-carpo phalangeal joint. There is only one phalangeal joint, modeled as a revolute joint; see Fig. 4. The kinematics equations can be written as

$$\begin{aligned}\hat{Q}_{thumb} &= \hat{S}_{c0}(\theta_0)\hat{T}_{c12}(\theta_1,\theta_2)\hat{T}_{t45}(\theta_4,\theta_5)\\ &\quad \hat{T}_{t67}(\theta_6,\theta_7)\hat{S}_{t8}(\theta_8)\end{aligned} \tag{10}$$

To verify the kinematic model, dimensions from the literature are introduced in the model for each limk and a series of linear joint trajectories are generated. Some snapshots of the resulting motion of the hand are shown in Fig. 5. This model is considered an appropriate good approximation that provides a good description of the motion of the hand using a total of 28 joint parameters.

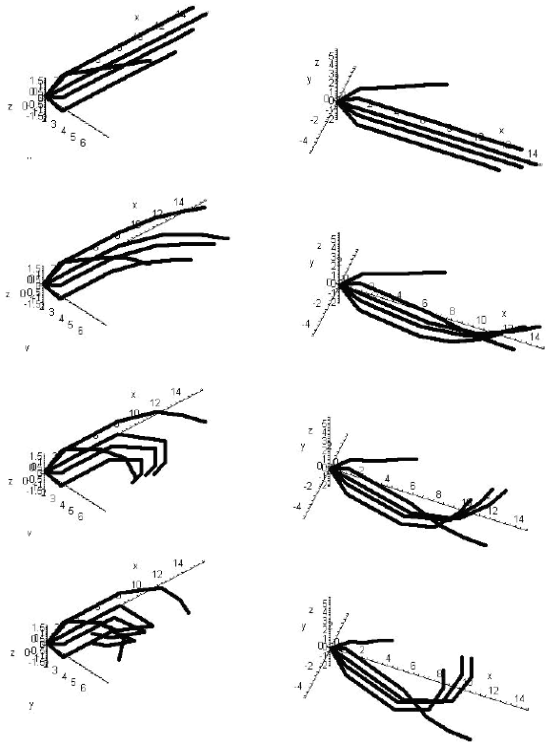

Fig.5. Simulation of the hand using the forward kinematic model

4. Kinematic Synthesis and Tracking for the Human Hand

4.1. Kinematic Synthesis

The kinematic synthesis for a serial chain defines the topology and dimensions of the chain that provide a desired motion of the end-effector. Dimensional synthesis assumes that the topology of the chain is specified and only its dimensions and joint variables are to be determined for a specified motion.

Several approaches to solve this problem have been developed; see for instance [13], [14] and [15]. Our approach follows Perez-Gracia and McCarthy [12], [16], who used a similar technique, using relative transformations and expressing the kinematics equations as Clifford algebra exponentials, known as dual quaternions.

The human skeleton presents a relatively high number of degrees of freedom. The dual quaternion approach provides with an efficient formulation of the design equations for these chains, which can be applied to the serial chains with any number of degrees of freedom.

4.2. Dimensional Synthesis using Clifford Algebra

The goal of this synthesis problem is to determine the dimensions and angle of the serial chains that can perform the motion given by real hand data.

Consider that the real hand data are defined as finite displacements $[P_j], j = 1,...,m.$ We choose $[P_1]$, the first frame, as the reference position and compute the relative displacements $[P_j][P_1^{-1}] = [P_{1j}], j = 2,...,n$ and express them as unit dual quaternions,

$$\hat{P}_{1j} = \cos\frac{\hat{\phi}_{1j}}{2} + \sin\frac{\hat{\phi}_{1j}}{2} P_{1j,}\ j = 2,...,n$$

The solution of the dimensional-synthesis problem is given by the values S_j and θ_j, $j = 1,...,m$, such that the displacement performed by the serial chain is equal to the datum displacement $\hat{P}_{1j,}$

$$\hat{P}_{1j} = e\frac{\Delta\hat{\theta}_{1j}}{2} s_1 e\frac{\Delta\hat{\theta}_{2j}}{2} s_2 ... e\frac{\Delta\hat{\theta}_{nj}}{2} s_n,\ j = 2,...,n. \tag{11}$$

For m datum displacements, the result is $8(m-1)$ design equations. The unknown are the m joint axes S_i, $i = 1,...,m$, and $m(n-1)$ pairs of joint parameters $\theta_{ij} + d_{ij}\varepsilon$.

It is easy to see that these equations become complicated quickly. If we wanted to solve for a single finger considering only positions of the fingertip, we would have 8x4=32 design parameters and 8 x (n-1) joint variables as unknowns; considering, in order to simplify the problem, that the motion of the last three joints is not independent, we would need 33 data positions in order to solve for 264 nonlinear equations.

Visual data from real hand motion presents the advantage that we may have information not only about the motion of the tip of the fingers, but also about the intermediate links. This allows us to apply the synthesis hierarchically [17], simplifying the solution process.

4.3. Hierarchical Synthesis

The solution for the serial chain of the index finger is presented in this section; the rest of the chains are solved similarly. The hierarchical synthesis process consists of solving sequentially link after link along the chain, starting from the base. We assume that we have data about the position of each differentiated link in the hand; see Fig. 6.

It is possible to attach a reference frame to the following hand sections, considering the lower arm as the base: $\hat{P}_{CMC}, \hat{P}_{PP}, \hat{P}_{MP}$ and $\hat{P}_{DP}$ for the carpal and metacarpal area, proximal, middle and distal phalanges. It is not likely that we will be able to separate the motion of the carpal and the metacarpal areas, so we consider them as a single body.

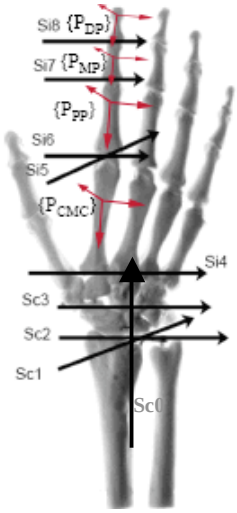

Fig. 6 Frames defining links along the index finger

The first step of the process consists of solving for the joints of (8),

$$\hat{S}_{c0}(\theta_0^i)\hat{T}_{c12}(\theta_1^i\theta_2^i)\hat{S}_{c4}(\theta_4^i) = \hat{P}_{CMC}^i,\ i = 1,...,n \tag{11}$$

so that they can perform the motion captured in $\hat{P}_{CMC}$. To fully establish the dimensions of the first three joints, $n = 5$ different positions are needed.

Once those are determined, solve for the next joint using the calculated result, which is denoted as $\hat{Q}_{0124}$, so that

$$\hat{T}_{i56}(\theta_5^i, \theta_6^i) = (\hat{Q}_{0124})^* \hat{P}_{PP}^i,\ i = 2,...,n, \tag{12}$$

where * denotes the conjugate dual quaternion. To solve for the carpo-metacarpal joint, at least $n = 3$ positions are needed. Use the appropriate solution to solve sequentially for the next two phalangeal joints,

$$\hat{S}_{i7}(\theta_7^i) = (\hat{Q}_{56}^i)^* (\hat{Q}_{0124}^i)^* \hat{P}_{MP}^i,$$
$$\hat{S}_{i8}(\theta_8^i) = (\hat{Q}_7^i)^* (\hat{Q}_{56}^i)^* (\hat{Q}_{0124}^i)^* \hat{P}_{DP}^i, \tag{13}$$

Each of these equations can be solved quickly when solved separately. The solution process is repeated for several datasets and the solutions are averaged to find the best approximation for the hand skeleton. The repeated solving process and averaging are necessary because of the lack of accuracy of the input data and of the rigid body model.

5. Solving Process

The kinematic synthesis equations obtained from the Clifford algebra exponentials cannot be solved exactly. The reasons for this are that the hand motion does not correspond exactly to the set of revolute joints, and also that the visual data contains inaccuracies. Instead, several points are considered and the problem is reformulated as an optimization problem in which we want to minimize the distance between the chain positions and the data. These equations are solved using a numerical Levenberg-Marquardt Nonlinear Least-Squares algorithm [19] implemented in C++ using Pentium4 3.2GHz, 512MB RAM. This algorithm does not guarantee convergence but the experimental results show a good behavior and fast solutions consistently; each joint takes milliseconds to be solved. From the solver we obtain both the location of the axes and the values of the joint variables. The axis parameters so obtained are used to find the twist angle between each axis and the link lengths (common normal distance between axes) that define the structure of the hand. The joint variables provide with a compact representation of the hand motion. The solving process is repeated each n captured frames, n being the minimum number of frames needed to determine the hand parameters.

6. Motion Tracking

The experimental setup for motion tracking consists of three black/white PC300XS cameras, whose orientation is at right angles to one another as shown in Fig.7. The camera calibration has been carried out with the help of [20]. Fig. 8 shows some calibration results.

The motion tracking system is based on tracking some points marked on a glove that the subject wears, see Fig. 9. The points are tracked by the motion-tracking algorithm written in MATLAB. The algorithm gives out the 3-D coordinates of the point of interest by stereo triangulation technique. The data obtained is to be used to define the three-dimensional position of each link.

7. Results

The solver has been tested with hand data generated using Maple. The values obtained from the solver show a very accurate match with our kinematic model of the hand, with a precision up to five decimal places for the artificially generated data. The joint motion of the model is divided into 100 equal parts. Set 1 in Tables 2-4 takes into account the 20^{th}, 40^{th}, 60^{th}, 80^{th} and 100^{th} values, set 2 in Tables 2-4 takes into account the 1^{st}, 15^{th}, 30^{th}, 50^{th} and 75^{th} values and set 3 in Tables 2-4 takes into account the 10^{th}, 25^{th}, 55^{th}, 85^{th} and 100^{th} values.

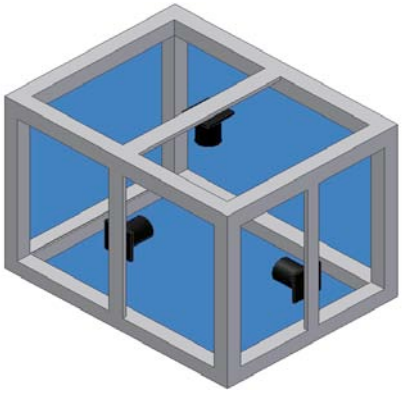

Fig. 7 Motion Tracking Setup

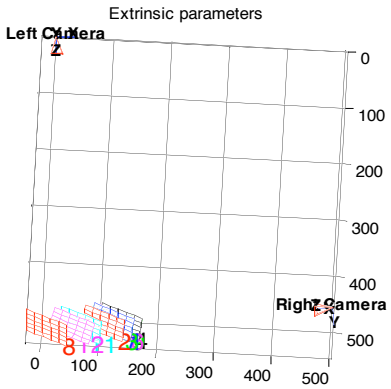

Fig. 8 Extrinsic Parameters of the calibration

Fig. 9 Hand Tracking

Table 2 shows the axis parameters obtained by solving the kinematic synthesis equations of the respective joints, where s0 denotes the coordinates of the axis Sc0 and c0 represents the coordinates of a point on the axis Sc0, and similarly for the rest of the axes. S_{mN} , N=4, 5, 6, 7 and 8 denote the axes of the middle finger and S_{cM} , M=0, 1 and 2 are the common wrist axes for all the fingers (see Annex A). Table 3 shows the calculated link lengths and link twist angles (see Annex B), where link01 represents the link length between axis 0 and 1, and so on, which do match with the D-H values as shown in Table 1. Table 4 shows the relative joint angles that define the motion of the hand, where alpha01represents the twist angle between axis 0 and 1, and similarly for the rest (see Annex C).

8. Conclusions

This paper presents a process to identify the motion of each degree of freedom of the human hand using a non-contact

method. The human hand is modeled as a series of chains using revolute joints, expressed as Clifford algebra exponentials. Using the kinematic synthesis approach, 3-D visual data obtained from three cameras can be used to determine both the dimensions of the hand and the rotation at each joint that determines the motion. The results obtained using data generated from the hand model shows that the solver returns accurate information for the hand motion. So far, the experimental data obtained from the cameras has been used to obtain some simplified results for the index finger. Future tasks include the use of the visual data for synthesizing the whole hand for any arbitrary motion.

This method is to be used as the input for the system identification of myoelectric signals, which will in turn be used to control a prosthetic hand. Current research on myoelectric signals considers unit basic hand actions that are in fact complex hand motions involving many degrees of freedom. It is our goal to identify and separate the commands for the motion of each independent degree of freedom, so that the prosthetic hand can have the richness of motion of the human hand.

REFERENCES

[1] Jingdong Zhao, Zongwu Xie, Li Jiang and Hegao Cai, "A Five-fingured Underactuated Prosthetic Hand Control Scheme*", First IEEE/RAS-EMBS Int. Conf. on Biomedical Robotics and Biomechatronics, Italy, February 20-22, 2006.

[2] L. Zollo, S. Roccella, R. Tucci, B. Siciliano, E. Guglielmelli, M.C. Carrozza and P. Dario, "Mechatronic Design and Control of an Anthropomorphic Artificial Hand for Prosthetics and Robotic Applications", First IEEE/RAS-EMBS Int. Conf. on Biomedical Robotics and Biomechatronics, Italy, February 20-22, 2006.

[3] C. Cipriani, F. Zaccone, G. Stellin, L. Beccai, G. Cappiello, M.C. Carrozza and P. Dario, "Closed-loop Controller for a Bioinspired Multi-fingered Underactuated Prosthesis", IEEE/RAS Int. Conf. on Robotics and Automation, Orlando, Florida, May 15-19, 2006.

[4] K. Hoshino and T. Tanimoto, "Real-Time Hand Posture Estimation without Deviation of Search Time", First IEEE/RAS-EMBS Int. Conf. on Biomedical Robotics and Biomechatronics, Italy, February 20-22, 2006.

[5] Sebastian Bitzer and Patrick van der Smagt, "Learning EMG Control of a Robotic Hand: Towards Active Prostheses", IEEE/RAS Int. Conf. on Robotics and Automation, Orlando, Florida, May 15-19, 2006.

[6] Mitja Veher and Tadej Bajd, "Assessment of Human Hand Kinematics", IEEE/RAS Int. Conf. on Robotics and Automation, Orlando, Florida, May 15-19, 2006.

[7] Karthikeyan. D, Obiajulu Isebor, Alba Perez, Marco P. Schoen and D. Subbaram Naidu, "Kinematic Synthesis for Smart Hand Prosthesis", First IEEE/RAS-EMBS Int. Conf. on Biomedical Robotics and Biomechatronics, Italy, February 20-22, 2006.

[8] R. Tubiana, "Examination of Hand and Wrist", 2nd edition, Martin Duntiz Ltd, 1996.

[9] D.A. Winter, "Biomechanics and Motor Control of Human Movement", 2nd edition, Wisley-Interscience, New York, 1990.

[10] V. Frankel et al.,"Basic Biomechanics of the Muscoskeletal System", 2nd edition, Lippincott Williams & Wilkins, 1989.

[11] J.M. Selig, "Geometrical Methods in Robotics", Springer-Verlag, New York, 1996.

[12] A. Perez and J.M. McCarthy, "Sizing a Serial Chain to Fit a Task Trajectory Using Clifford Algebra Exponentials", 2005 IEEE Int. Conf. on Robotics and Automation, Barcelona, April 18-22, 2005.

[13] L.W. Tsai and B. Roth, "Design of Dyads with Helical, Cylindrical, Spherical, Revolute and Prismatic Joints", Mechanism and Machine Theory, 7:591-598, 1972.

[14] C.H. Suh and C.W. Radcliffe, "Kinematics and Mechanisms Design", John Wiley & Sons, New York, 1978.

[15] E. Lee and C. Mavroidis, "Geometric Design of 3R Manipulators for Reaching Four End-Effector Spatial Poses", the Int. Journal of Robotics Research, 23(3): 247-254, 2004.

[16] A. Perez-Gracia and J.M. McCarthy, "Kinematic Synthesis of Spatial Serial Chains Using Clifford Algebra Exponentials", Proc. ImechE Vol. 220 Part C: Journal of Mechanical Engineering Science, 2006 (in press).

[17] M.C. Villa-Uriol, F. Kuester, N. Bagherzadeh, A. Perez and J.M. McCarthy, "Kinematic Synthesis of Avatar Skeletons from Visual Data", Advances in Robot Kinematics, J. Lenarcic and C. Galletti,eds., Klower Academic Publishing, 2004.

[18] S. Van Sint Jan, D.J. Guirintano, D.E. Thompson and M. Rooze, "Joint Kinematics Simulation from Medical Imaging Data", IEEE Transactions on Biomedical Engineering, 44(12): 1175-1180, 1997.

[19] http://www.ics.forth.gr/~lourakis/levmar/

[20] http://www.vision.caltech.edu/bouguetj/calib_doc/

[21] Donald A. Neumann, "Kinesiology of the Musculoskeletal System", Mosby, Philadelphia, 2002.

[22] Ben Pansky and Earl Lawrence House, "Review of Gross Anatomy", 3rd edition, Macmillan Publishing Company, New York, 1975.

ANNEX A

Table 2. Axis parameters from the solver

	Set 1 **20,40,60,80 and 100**	Set 2 **1,15,30,50 and 75**	Set 3 **10,25,55,85 and 100**
Axis S_{c0}	s0=[1,0,0], c0=[-16.6,0,0]	s0=[1,0,0], c0=[-5.929,0,0]	s0=[-1,0,0], c0=[-9.125,0,0]
Axis S_{c1}, S_{c2}	s1=[0,0.387,-0.921], s2=[0.467,0.814,0.342], c1=c2=[0,0,0]	s1=[0,0,-1], s2=[0.707,0.707,0], c1=c2=[0,0,0]	s1=[0,0.187,-0.982] s2=[-0.600,-0.785,-0.149] c1=c2=[0,0,0]
Axis S_{m4}	s4=[-0.054,-0.360,0.931], c4=[2.706,0.281,-4.367]	s4=[0.061,-0.061,0.996], c4=[1.771,-1.771,-3.497]	s4=[0.0132,-0.197,0.980], c4=[2.192,-0.950,-3.801]
Axis S_{m5}, S_{m6}	s5=[-0.054,-0.360,0.931], s6=[-0.187,-0.912,-0,363], c5=c6=[6.327,-3.109,-.830]	s5=[0.061,-0.061,0.996]; s6=[0.707,0.707,0],c5=c6= [5.001,-5.001,-0.618]	s5=[0.013,-0.197,0.980], s6=[0.481,0.860,0.166], c5=c6=[5.717,-4.111,-0.904]
Axis S_{m7}	s7=[0.022,0.366,-0.930], c7=[9.071,-14.932,27.404]	s7=[-0.147,0.147,-0.978], c7=[6.125,-6.125,-9.974]	s7=[0.083,-0.233,0.968], c7=[6.888,-0.393,-23.505]
Axis S_{m8}	s8=[-0.022,-0.366,+0.930], c8=[11.963,-10.300,15.175]	s8=[0.147,-0.147,0.978], c8=[9.920,-10.558,5.082]	s8=[0.083,-0.233,0.968], c8=[11.592,-8.630,4.926]

ANNEX B

Table 3. Link length and angle between axes

	Set 1 **20,40,60,80 and 100**	Set 2 **1,15,30,50 and 75**	Set 3 **10,25,55,85 and 100**
Axis S_{c0}			
Link length, twist angle	0	0	0
Axis S_{c1}, S_{c2}			
Link length, twist angle	link01=0cm,link12=0cm alpha01=1.5707radians aplha12=1.5707radians	link01=0cm, link12=0cm alpha01=1.5707radians alpha12=1.5707radians	link01=0cm, link12=0cm alpha01=1.5707radians alpha12=1.5707radians
Axis S_{m4}			
Link length, twist angle	link24=2.799cm alpha24=1.5707radians	link24=2.799cm alpha24=1.5707radians	link24=-2.799cm alpha24=1.5707radians
Axis S_{m5}, S_{m6}			
Link length, twist angle	link45=4.299cm link56=0cm alpha45=0radians alpha56=1.5707radians	link45=4.300cm link56=0cm alpha45=0radians alpha56=1.5707radians	link45=4.300cm link56=0cm alpha45=0radians alpha56=1.5707radians
Axis S_{m7}			
Link length, twist angle	link67=3.500cm alpha67=1.57079radians	link67= 3.500cm alpha67=1.57079radians	link67=3.500cm alpha67=1.57079radians
Axis S_{m8}			
Link length, twist angle	link78=2.599cm alpha78=0radians	link78=2.599cm alpha78=Pi radians	link78=2.600cm alpha78=0radians

ANNEX C

Table 4. Relative joint angles for each joint

	Set 1 **20,40,60,80 and 100**		Set 2 **1,15,30,50 and 75**		Set 3 **10,25,55,85 and 100**	
Axis S_{c0} **Relative θ values**	Θ 0		θ 0		θ 0	
	θ1=0.418 θ2=0.837 θ3=1.256 θ4=1.675		θ1=0.293 θ2=0.607 θ3=1.026 θ4=1.549		θ1=-0.314 θ2=-0.942 θ3=-1.570 θ4=-1.884	
Axis S_{c1}, S_{c2} **Relative θ values**	θ 1	θ 2	θ 1	θ 2	θ 1	θ 2
	θ1=-0.314 θ2=-0.628 θ3 =-0.94 θ4=-1.256	θ1=-0.157 θ2=-0.314 θ3=-0.471 θ4=-0.628	θ1=-0.219 θ2=-0.455 θ3=-0.769 θ4=-1.162	θ1=-0.109 θ2=-0.227 θ3=-0.384 θ4=-0.581	θ1=-0.235 θ2=-0.706 θ3=-1.178 θ4=-1.413	θ1=0.117 θ2=0.352 θ3=0.589 θ4=0.706
Axis S_{m4} **Relative θ values**	θ 4		θ 4		θ 4	
	θ1=0.034 θ2=0.069 θ3=0.104 θ4=0.139		θ1=0.024 θ2=0.050 θ3=0.085 θ4=0.129		θ1=0.026 θ2=0.078 θ3=0.130 θ4=0.157	
Axis S_{m5}, S_{m6} **Relative θ values**	θ 5	θ 6	θ 5	θ 6	θ 5	Θ 6
	θ1=0.279 θ2=0.558 θ3=0.837 θ4=1.117	θ1=0.094 θ2=0.188 θ3= 0.282 θ4= 0.376	θ1=0.195 θ2=0.404 θ3=0.684 θ4=1.032	θ1=-0.065 θ2=-0.136 θ3=-0.230 θ4=-0.348	θ1=0.209 θ2=0.628 θ3=1.047 θ4=1.256	θ1=-0.070 θ2=-0.212 θ3=-0.353 θ4=-0.424
Axis S_{m7} **Relative θ values**	Θ 7		θ 7		θ 7	
	θ1=-0.314 θ2=-0.628 θ3=-0.942 θ4=5.026		θ1=-0.219 θ2=-0.455 θ3=-0.769 θ4=5.120		θ1=0.235 θ2=0.706 θ3=-5.105 θ4=-4.869	
Axis S_{m8} **Relative θ values**	Θ 8		θ 8		θ 8	
	θ1=-0.314 θ2=-0.628 θ3=5.340 θ4=-1.256		θ1=0.219 θ2=0.455 θ3=0.769 θ4=1.162		θ1=0.235 θ2=0.706 θ3=1.178 θ4=1.413	